Chem. Senses 31: 821–834, 2006
doi:10.1093/chemse/bjl025
Advance Access publication September 19, 2006

Glomerular Targets of *Heliothis subflexa* Male Olfactory Receptor Neurons Housed within Long Trichoid Sensilla

Seong-Gyu Lee[1], Neil J. Vickers[2] and Thomas C. Baker[1]

[1]Department of Entomology, Chemical Ecology Laboratory, Pennsylvania State University, University Park, PA 16802 USA and [2]Department of Biology, University of Utah, Salt Lake City, UT 84112 USA

Correspondence to be sent to: Thomas C. Baker, Department of Entomology, Chemical Ecology Lab, Pennsylvania State University, University Park, PA 16802 USA. e-mail: tcb10@psu.edu

Abstract

We used single-sensillum recordings to characterize male *Heliothis subflexa* antennal olfactory receptor neuron physiology in response to compounds related to their sex pheromone. The recordings were then followed by cobalt staining in order to trace the neurons' axons to their glomerular destinations in the antennal lobe. Receptor neurons responding to the major pheromone component, (*Z*)-11-hexadecenal, in the first type of sensillum, type-A, projected axons to the cumulus of the macroglomerular complex (MGC). In approximately 40% of the type-A sensilla, a colocalized receptor neuron was stained that projected consistently to the posterior complex 1 (PCx1), a specific glomerulus in an 8-glomerulus complex that we call the Posterior Complex (PCx). We found that receptor neurons residing in type-B sensilla and responding to a secondary pheromone component, (*Z*)-9-hexadecenal, send their axons to the dorsal medial glomerulus of the MGC. As in the type-A sensilla, we found a cocompartmentalized neuron within type-B sensilla that sends its axon to a different glomerulus of the PCx4. One neuron in type-C sensilla tuned to a third pheromone component, (*Z*)-11-hexadecenol, and a colocalized neuron responding to (*Z*)-11-hexadecenyl acetate projected their axons to the anteromedial and ventromedial glomeruli of the MGC, respectively.

Key words: cobalt staining, glomerulus, macroglomerular complex, olfactory receptor neuron, posterior complex, single-sensillum recording

Introduction

Heliothis subflexa (Lepidoptera, Noctuidae) larvae are known to feed on plants in the genus *Physalis*, such as ground cherry. In Mexico, *H. subflexa* larval feeding on tomatillos can be so extensive that it is now considered to be a pest of this agricultural crop (Mitter et al. 1993). Even though they are not yet serious agricultural pests in the United States, the successful hybridization of *H. subflexa* with the well-known pest species, *Heliothis virescens*, has interested researchers as a potential control technique for *H. virescens* because hybrid male offspring are sterile, as are backcross males (Laster 1972; Sheck and Gould 1995, 1996; Teal and Oostendorp 1995).

Morphological and molecular phylogenies of heliothine moths are in agreement that these 2 species are closely related (Mitter et al. 1993; Cho et al. 1995; Fang et al. 1997). They are sympatric in North America and share the same female-emitted major pheromone component, (*Z*)-11-hexadecenal (Z11-16:Ald) (Roelofs et al. 1974; Tumlinson et al. 1975; Klun et al. 1979, 1980, 1982). However, interspecific attraction of males and cross-mating do not occur in nature due to the presence of different minor pheromone components in the blends of the 2 species. *Heliothis subflexa* females release (*Z*)-9-hexadecenal (Z9-16:Ald) and (*Z*)-11-hexadecenol (Z11-16:OH) (Teal et al. 1981; Heath et al. 1991) as minor components that significantly increase attraction of *H. subflexa* males and are therefore part of this species' sex pheromone blend (Heath et al. 1990; Vickers 2002). Hexadecenal (16:Ald), (*Z*)-11-hexadecenyl acetate (Z11-16:Ac), (*Z*)-9-hexadecenyl acetate (Z9-16:Ac), (*Z*)-7-hexadecenyl acetate (Z7-16:Ac), and (*Z*)-9-hexadecenol (Z9-16:OH) have been identified as other constituents in the female pheromone gland (Teal et al. 1981; Klun et al. 1982; Heath et al. 1991), but as yet these compounds have not been shown to play a pheromonal role.

Another sympatric heliothine pest, *Helicoverpa zea*, like *H. subflexa,* emits Z11-16:Ald and Z9-16:Ald as essential pheromone components for male attraction (Pope et al. 1984; Vetter and Baker 1984). However, the *H. subflexa*

blend will not attract *H. zea* males because the Z11-16:OH present in this blend has been shown to be antagonistic to *H. zea* attraction when added to its pheromone blend (Shaver et al. 1982; Quero and Baker 1999).

Much work has now been performed on the sex pheromone olfactory systems of these 3 North American heliothine moth species. These studies include examination of the electrophysiological response profiles of the olfactory receptor neurons (ORNs) (Almaas et al. 1991; Berg et al. 1995; Cossé et al. 1998; Baker et al. 2004; Lee et al. 2006) as well as neuroanatomical studies of the central nervous system pathways that integrate and relay the inputs from the ORNs (Christensen et al. 1991, 1995; Vickers et al. 1998; Vickers and Christensen 2003). Neuroanatomical studies of the ORN pathways into the antennal lobe, the first integrative center of the moth olfactory system, also now have begun to delineate exactly how ORN pheromone component–specific information converges onto specific glomeruli (knots of neuropil within which synaptic contacts are made between ORNs and central neurons) as well as how pheromone blend quality information is conveyed to higher centers by central olfactory projection neurons.

Such studies have been illuminating and have for instance shown how the pheromone component–tuned ORNs of *H. virescens* (Berg et al. 1998), *Helicoverpa assulta* (Berg et al. 2005), and *H. zea* (Lee et al. 2006) project their axons to component-specific homologous glomeruli in these species' macroglomerular complexes (MGCs). However, similar information about the ORNs of *H. subflexa* has been lacking. We therefore sought to clarify the primary ORN pathways to the MGC for *H. subflexa* by using the ORN cobalt-staining technique that has proven to be so informative for other noctuid moth species (Hansson et al. 1992; Hansson 1995; Ochieng et al. 1995; Todd et al. 1995; Berg et al. 1998, 2005; Lee et al. 2006).

We report here that the glomeruli in which male *H. subflexa* component-specific ORNs arborize correspond well to the glomerular arborization locations of similarly tuned projection interneurons exiting the *H. subflexa* antennal lobe to higher centers (Vickers and Christensen 2003). In addition, we found that the ORNs (Lee et al. 2006) that are cocompartmentalized with ORNs tuned to Z11-16:Ald or to Z9-16:Ald project their axons to a cluster of glomeruli located just posterior to the MGC, which we call the Posterior Complex (PCx) (Lee et al. 2006). The ORNs colocalized with Z11-16:Ald–sensitive ORNs always project to the same glomerulus, the PCx1, in the PCx, and the ORNs cocompartmentalized with Z9-16:Ald–sensitive ORNs always project to a different glomerulus in this complex, the PCx4.

Materials and methods

Insects

A colony of *H. subflexa* was maintained at the University of Utah as described by Vickers (2002). Pupae were separated according to sex and shipped overnight to the Baker laboratory. Emerging adults were segregated into separate cages daily to obtain individuals of known age. Adults were maintained on a 16:8 light:dark photoperiod at 25 °C, 40–50% relative humidity.

Chemical stimuli

Five heliothine moth sex pheromone compounds were utilized to identify sensillar types according to Baker et al. (2004). The synthetic compounds, Z11-16:Ald, Z9-16:Ald, (*Z*)-9-tetradecenal (Z9-14:Ald), Z11-16:Ac, and Z11-16:OH were purchased from Bedoukian Research Inc. (Danbury, CT; purities >98% verified by gas chromatography). Serial dilutions were made in high performance liquid chromatography-grade hexane to 0.1 μg/μl and 1 μg/μl and stored at −20 °C. To prepare stimulus cartridges for each compound, 10 μl of each diluted solution was loaded onto a 0.7 × 2.5–cm filter paper strip, the solvent allowed to evaporate, and then the paper strip was placed in a glass Pasteur pipette (2.5 ml). For the mixture of Z11-Ald and (±)-linalool, 10 μg (±)-linalool (97%; Aldrich Chemical Company, Milwaukee, WI) in 10 μl hexane was added to a filter paper onto which 10 μg Z11-16:Ald had already been loaded, and the solvent was allowed to evaporate.

New cartridges were prepared every 5 days and stored at −20 °C when not in use after being sealed with aluminum foil.

Single-sensillum recording

The cut-sensillum technique (Kaissling 1974; Van der Pers and Den Otter 1978; Cossé et al. 1998) was used to record the activities of ORNs housed within individual antennal sensilla. A male *H. subflexa* was restrained inside a disposable pipette tip; the narrow end of the tip was cut to enlarge it to allow the male's head to pass through. The head and antennae were immobilized in the proper orientation using dental wax. A Ag/AgCl wire was inserted into the abdomen to serve as a ground and was then secured with an alligator clip attached in turn to the end of one of the micromanipulators. By maneuvering this micromanipulator, the tip of one of the many sexually dimorphic long trichoid sensilla was placed on the edge of a vertically positioned metal knife fashioned by sharpening an insect pin. The sensillum tip was cut off using a horizontally positioned glass knife held in place by a second micromanipulator. The cut end of the sensillum was then contacted first by a saline-filled glass micropipette and a connection established in order to determine the type of sensillum that was contacted, according to the differential responses of the ORNs to the array of pheromone odorants. The AC signals from the ORNs were amplified using a high-impedance amplifier (DAM50, World Precision Instruments, Sarasota, FL), and the action potentials were digitally recorded directly onto a PC by means of data processing software (Syntech Autospike 3.2; Hilversum, The Netherlands).

Volatile stimuli (50-ms pulses at 40 ml/s flow rate) were delivered into a continuous charcoal-filtered humidified airstream (~15 ml/s) by means of a stimulus flow-controller device (SFC-2; Syntech). The odor-laden air pulse passed through a 14-cm-long glass tube (8 mm inner diameter) whose outlet was positioned 2 cm from the antenna. Linear flow speed through this continuous airstream was ~0.3 m/s.

Staining of ORNs with cobalt-lysine

We used a cobalt-lysine–staining technique, with a minor modification, following the protocol of Hansson et al. (1995), Ochieng et al. (1995), and Todd et al. (1995) in order to try to find the glomerular arborization destinations of the axons of each electrophysiologically identified ORN. A glass electrode filled with 0.5 M cobalt-lysine solution replaced the saline recording electrode after the ORNs residing in the sensillum were characterized using the saline electrode to discern their response specificity. The cobalt-lysine electrode then was used to contact the sensillum for 10 min, during which time one of the pheromone-related compounds to which one of the ORNs was tuned was puffed at a frequency of 0.7 Hz. Unlike in other noctuid moth species, the uptake of cobalt by heliothine moth ORNs is either not activity-dependent or occurs as a result of the ORNs' spontaneous activities alone (Lee et al. 2006). Nevertheless, we wanted to try to increase the chances for successful cobalt uptake by inducing the ORNs to fire in response to repetitive odorant stimulus puffs (Hansson et al. 1992; Todd et al. 1995). For these repetitive stimulations to type-A sensilla, 10 μg Z11-16:Ald or a mixture of 10 μg Z11-16:Ald plus 10 μg (±)-linalool was used. For type-B sensilla, only 10 μg Z9-16:Ald was used, and for type-C sensilla, 10 μg Z11-16:Ac, 10 μg Z11-16:OH, or blank cartridges were used.

The male was then removed from the electrophysiology rig and refrigerated for 2 days at 4 °C to allow sufficient time for the cobalt to migrate along the axons to the antennal lobe. The brain was then dissected from the head in saline (150 mM NaCl, 3 mM KCl, 3 mM $CaCl_2$, 10 mM N-Tris (hydroxymethyl)methyl-2-aminoethanesulfonic acid, and pH 7.0) and treated with ammonium sulfide solution for the cobalt precipitation step. Brains were washed 4 times for 5 min each with saline that included 2% sucrose. After fixation, any cobalt-stained ORNs' axons were intensified with silver (Bacon and Altman 1977). Brains were dehydrated through a graded series of ethanol, cleared with methyl salicylate, and viewed as whole mounts under a light microscope. All brains were stored at 4 °C in 70% alcohol until being used for the next procedure.

Brains were preliminarily counterstained for differentially enhancing cell bodies and glomeruli using modified Lee's methylene blue-basic fuchsin solution (Bennett et al. 1976; Lee et al. 2006). Our modified solution used 0.5% methylene blue + 0.5% azure II in 1% borate: 0.5% basic fuchsin in 95% ethanol: 100% ethanol = 1:2:1—or 0.15% methylene blue, 0.15% azure II, and 0.3% basic fuchsin in 70% alcohol for 10 min. The stained whole brains were washed with 70% alcohol and dehydrated sequentially with 95%, pure ethanol (twice), and twice with propylene oxide. The infiltration procedure was then performed using a mixture of propylene oxide and Durcupan resin (Sigma-Aldrich, St Louis, MO). The propylene oxide was allowed to evaporate at room temperature (RT) overnight, and then the brains were embedded in pure Durcupan resin. Most brains were oriented for frontal sections, but a few were prepared specifically for horizontal sections. After curing at 60 °C for 2 days, brains were sectioned at a thickness of 10 μm.

Immunocytochemistry

For better interpretation of 3-dimensional (3D) glomerular topography, confocal microscopic images were collected after immunocytochemical stainings of glomeruli and then reconstructed to a 3D image (Figure 2D). We used a monoclonal anti-synaptotagmin of *Drosophila* from mouse as a primary antibody and goat anti-mouse immunoglobulin G antibody conjugated with Alexa Fluo555 (Molecular Probe, Eugene, OR) as secondary antibody. The anti-synaptotagmin antibody developed by Dr Kai Zinn was obtained from the Developmental Studies Hybridoma Bank developed under the auspices of the National Institute of Child Health and Human Development and maintained by The University of Iowa, Department of Biological Sciences, Iowa City, IA. Brains were dissected in 4% paraformaldehyde in phosphate-buffered saline (PBS) with 0.2% Triton X-100 (PBST) and washed with PBST 4 times for 30 min at RT. After washing, brains were preincubated in 5% normal goat serum (NGS) in 0.5% PBST overnight at 4 °C and then incubated in primary antibody (1:100 in 2% NGS PBST) for 3 days at 4 °C. Brains were washed for 6 h at RT and then washed with PBST overnight at 4 °C and then incubated in secondary antibody (1:100 in 2% NGS PBST) for 3 days at 4 °C, always in darkness from this procedure. After washing with PBST for 6 h at RT and then washing overnight at 4 °C and with PBS 3 times for 1 h each at RT, brains were dehydrated through a graded series of ethanol and cleared with methyl salicylate. They were then observed using a 1 or 2 μm thickness of optical sections with the laser scanning confocal microscope (Olympus Fluoview 300, Olympus America Inc., Melville, NY) housed in the Huck Institutes for the Life Sciences at Pennsylvania State University. Alexa Fluo555 was excited with a green HeNe laser (543 nm) and images collected through a 565 long-pass filter.

Image processing and figure preparation

Histological sections of cobalt-stained brains were captured with Spot RT II digital camera (Diagnostic Instrument, Sterling Heights, MI) attached to a compound microscope (Olympus BX50). The color, brightness, and contrast levels of digitally captured images were adjusted using Adobe Photoshop 7.0 (Adobe Systems, San Jose, CA) for better

contrast. Schematic diagrams of Figure 2A,B,C were digitally drawn using Canvas 9 (ACD Systems, Miami, FL). Captured images of confocal microscopy were reconstructed (Figure 2D) using software developed by JC Fiala and KM Harris (downloaded from www.synapses.bu.edu).

Results

Our histological examinations of the *H. subflexa* antennal lobe (Figure 1) revealed an MGC the same as described by Vickers and Christensen (2003), comprised of 4 glomeruli called the cumulus (Cu), the dorsomedial (DM), the anteromedial (AM), and the ventromedial (VM) (Figures 1 and 2). There were also numerous ordinary glomeruli clearly set apart from the 4 MGC glomeruli. In addition, we also found a distinct cluster of 8 glomeruli just posterior to the MGC in every male that we examined, and we named this the Posterior Complex (PCx) (Figures 1 and 2). Many of the PCx glomeruli lie in the most posterior area of this most dorsal portion of the antennal lobe (Figure 1). The PCx is also clearly separated from the large cluster of ordinary glomeruli (Figures 1 and 2). A large bundle of fibers projects out of the PCx, the main trunk of which is a confluence of the bundles from the various levels all oriented toward the center of the antennal lobe (Figures 1B and 2C). The fiber bundle from the PCx eventually merges with the bundle from the MGC (Figure 2C). The *H. subflexa* PCx appears similar to the PCx described for the first time in *H. zea* (Lee et al. 2006), except that the *H. subflexa* PCx has one more glomerulus than does *H. zea*. The numbers we assigned to the PCx glomeruli were determined as for *H. zea*, according to the order of their dorsal to ventral, anterior to posterior, and medial to lateral positions, respectively, after examining serial sections from 12 males (16 antennal lobes). The PCx morphology and topography were confirmed by the 3D reconstruction images (Figure 2D) obtained from serial 1- or 2-μm-thick optical sections from 8 antennal lobes (ALs) using laser scanning confocal microscopy. These reconstructions could be performed without the arbitrary reorientation of physical microtome sections as was required for reconstructing the antennal lobes in our cobalt-staining studies.

Type-A sensilla

We attempted to stain type-A sensilla, as determined by their electrophysiological profiles in which ORN action potentials occurred only in response to the major pheromone component, Z11-16:Ald (Figure 3A) (Baker et al. 2004). Among the 72 such sensilla that were located, 28 produced successfully stained preparations showing arborizations in the antennal lobe. Out of these 28 preparations, 17 (60.7%) exhibited a single axonal stain projecting exclusively to the largest of the MGC glomeruli, the Cu (Figure 1, Table 1).

The other 11 preparations (39.3%) exhibited 2 or more stained ORNs (Table 1). Without exception, one of these axons projected to the Cu and a second axon projected to the most dorsal of the PCx glomeruli, which we have labeled "PCx1" (Figures 3 and 4).

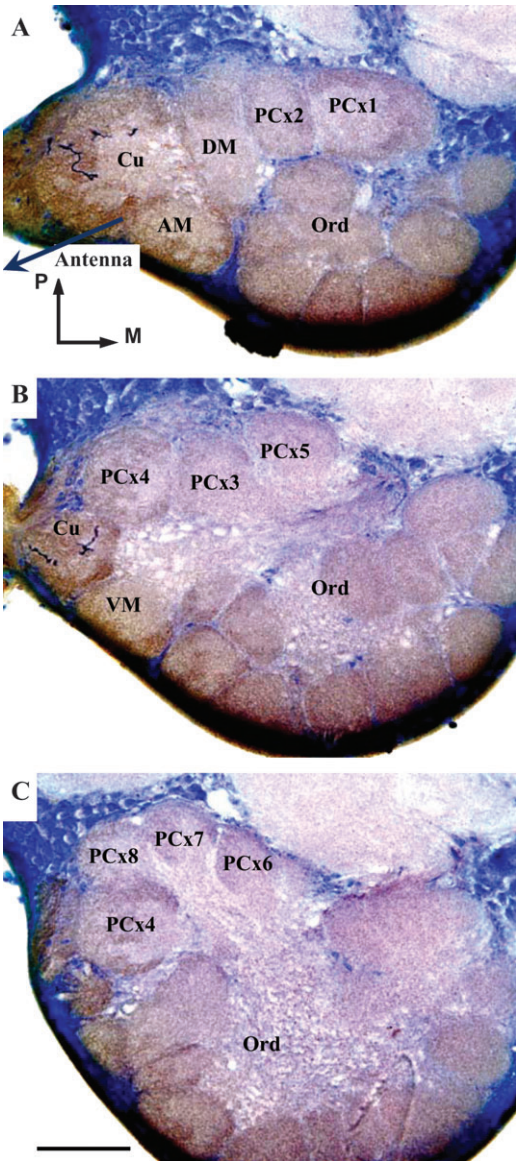

Figure 1 Dorsal view the antennal lobe of *Heliothis subflexa* brain (horizontal sections) showing position of the PCx relative to MGC and ordinary glomeruli (Ord). **(A)** A section at a depth of 60 μm from the most dorsal surface. Three MGC compartments (Cu, DM, and AM) and 2 glomeruli of the PCx (PCx1 and 2) are visible. A stained axon's arborizations are visible in the Cu. **(B)** Depth of 80 μm showing the Cu (again with stained arborizations) and VM of the MGC and 3 more glomeruli of the PCx (PCx3, 4, 5). **(C)** A depth of 110 μm (a more ventral section) showing 4 glomeruli of the PCx (PCx4, 6, 7, 8). Ord, ordinary glomeruli; P, posterior; M, medial. Scale bar = 50 μm.

An additional 2 sensilla out of those exhibiting projections to the Cu and PCx1 showed 2 or 3 extra axons projecting into ordinary glomeruli (Figure 4B,C). Also, an additional preparation exhibiting ORNs projecting to the Cu and PCx1 had its third axon projecting to the PCx4 of the PCx (Table 1).

Stimulation with repetitive puffs of either 10 μg Z11-16:Ald or a blend of 10 μg Z11-16:Ald and 10 μg linalool during

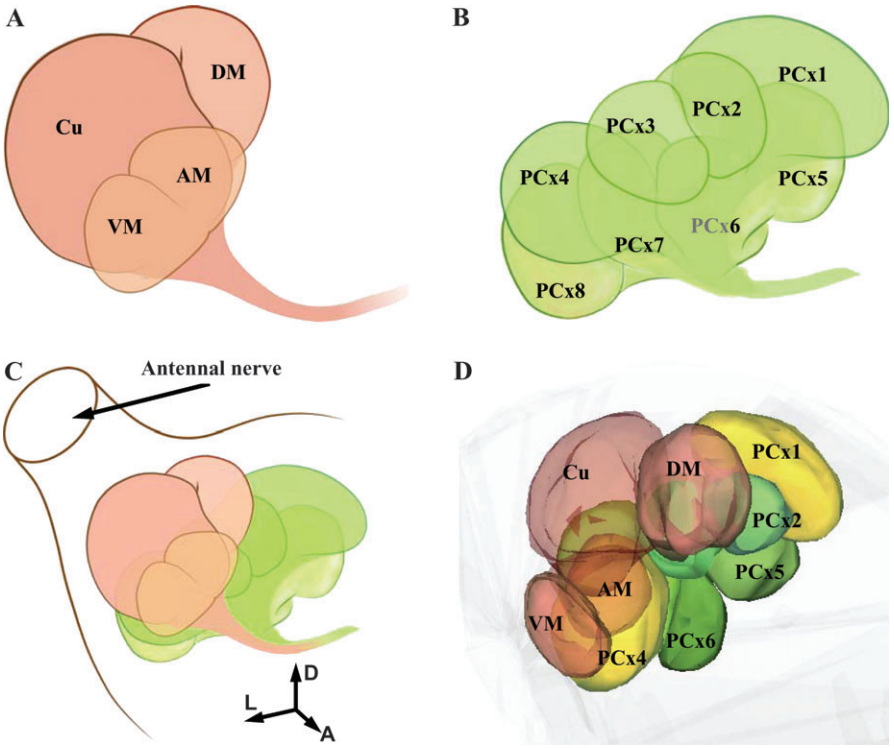

Figure 2 Schematic frontal view diagram of the glomerular topographies of the MGC and the PCx in the male *Heliothis subflexa* AL. **(A)** The MGC is comprised of 4 glomeruli; Cu, DM, AM, and VM glomeruli. **(B)** The PCx is comprised of 8 glomeruli, PCx1–8. The numbers after "PCx" are designated by the order of the glomerular arrangement in the AL; dorsal to ventral, anterior to posterior, and medial to lateral. The PCx1 glomerulus is positioned most dorsally in this complex and is the arborization location of the colocalized ORN from the type-A sensilla. The PCx4 glomerulus is positioned anteroventrally and is the destination of the colocalized ORN of type-B sensilla. **(C)** A combined view showing that the PCx is situated posterior to the MGC. Outgoing neurons from both the MGC and the PCx appear to form a common tract. **(D)** Three-dimensional reconstruction image from the series of optical sections with laser scanning confocal microscopy after fluorescence immunostaining for synapse-specific proteins. D, dorsal; L, lateral; A, anterior.

contact with the cobalt-filled electrode did not significantly influence the selective uptake of cobalt stain by the ORNs in these type-A sensilla. Adding linalool to Z11-16:Ald was tried here to see if the heightened firing of the large-spiking ORN caused by the addition of this plant volatile (Ochieng and Baker 2002) would enhance cobalt uptake. However, the ORNs of heliothine moths appear to take up stain spontaneously, without the need for odor stimuli to be presented, perhaps due to spontaneous background firing (Berg et al. 1998; Lee et al. 2006). Therefore again, approximately 60% of the stained type-A sensillar preparations, regardless of stimulus, ended up with a single-stained ORN projecting to the Cu with the remaining 40% exhibiting 2 stained ORNs with the second ORN projecting to PCx1.

The second ORN in type-A sensilla that is colocalized with the ORN responding to Z11-16:Ald does not reliably respond to any odorant, either taken from a panel of over 60 general and plant odorants or from an array of heliothine moth pheromone-related compounds (Lee 2006).

Type-B sensilla

Type-B sensilla were identified by their characteristic ORN responsiveness to Z9-16:Ald, an important minor pheromone component of this species, plus a low degree of cross-responsiveness to Z9-14:Ald (Figure 5A) (Baker et al. 2004). Spontaneous activities in clean air showed spikes having 2 distinct waveforms. The larger spiking of these ORNs showed a more symmetrically bipolar waveform than the smaller spiking ORN (Figure 5A). Responses during stimulation showed that it is this larger spiking ORN that is sensitive to Z9-16:Ald and Z9-14:Ald stimulation (Figure 5A) (Baker et al. 2004). The second ORN, the one having the more asymmetric, unipolar action potential, showed no consistent activity in response to any of our test compounds (Figure 5A) (Baker et al. 2004; Lee 2006).

We obtained 28 successful stains from ORNs in type-B sensilla in 58 preparations. The majority of these, 23 out of 28 (82.1%), resulted in 2 or more stained ORNs. In all cases, the 2 axons arborized in 2 specific glomeruli, the DM and the PCx4 (Table 1, Figures 2 and 5B). Eighteen of the 23 exhibited only 2 stained axons projecting to these 2 locations. The remaining 5 of these 23 exhibited an additional third or even a fourth stained ORN projecting either to an ordinary glomerulus (Figure 6A) or to the Cu (Table 1).

The ORNs from the remaining 5 out of 28 stained type-B sensillar preparations (~18%) showed only a single stained

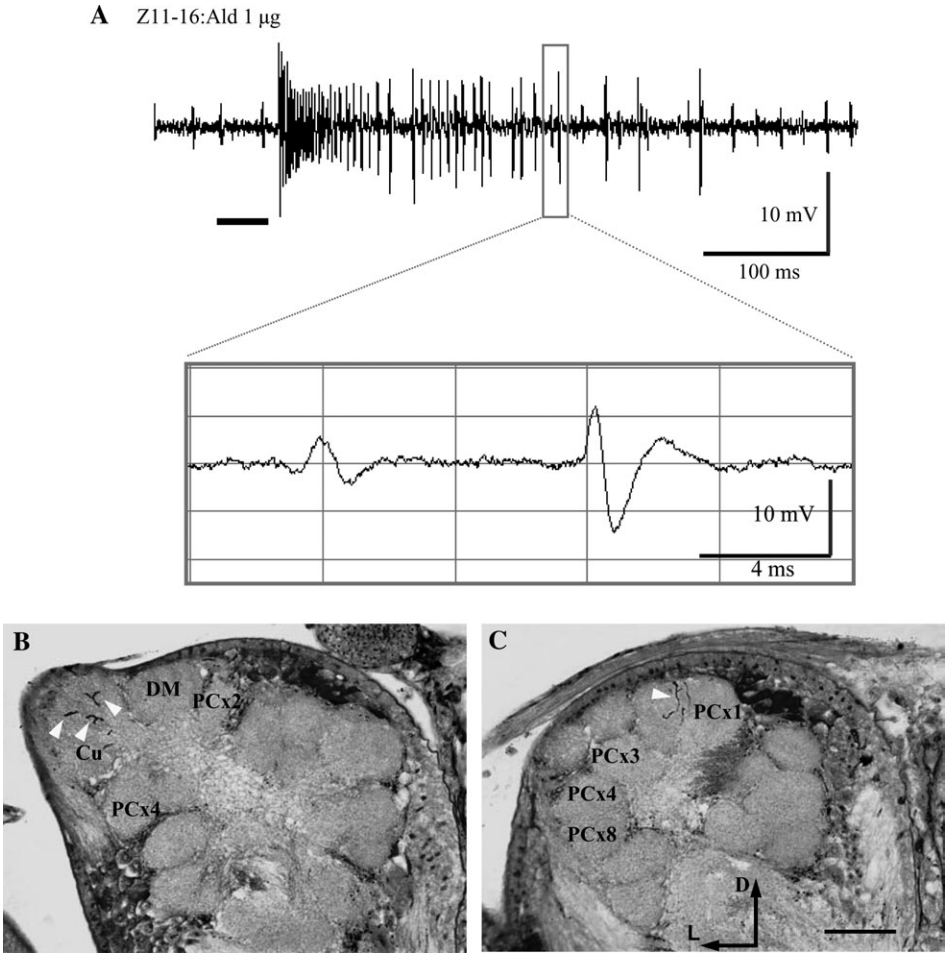

Figure 3 **(A)** Spike train of an ORN from a type-A sensillum in response to Z11-16:Ald puffed for 50 ms. Larger amplitude action potentials were elicited only by stimulation with Z11-16:Ald among test compounds used for the identification. A neuron with small spontaneous action potentials was not responsive consistently to any of the test compounds. Inset shows different waveforms from 2 different neurons; smaller action potential from a colocalized neuron and larger action potential from Z11-16:Ald–responsive ORN. **(B–C)** Frontal view of a male *Heliothis subflexa* antennal lobe showing the arborization destinations of 2 neurons that were stained within one type-A sensillum. (B) One stained axon arborized (arrowheads) in the Cu. (C) A second axon arborized (arrowhead) in the dorsal most glomerulus (PCx1) of the PCx. The section in (B) is 80 μm posterior from the frontal surface. The section in (C) is 40 μm posterior to (B). D, dorsal; L, lateral. Scale bar = 50 μm.

ORN (Table 1). One such ORN had its single axon projecting only to the PCx4, and the ORNs from the other 4 sensilla stained only the DM. One of the DM-targeting sensilla had one or 2 extra axon(s) that were stained in the antennal nerve, but the stains faded out before reaching a target glomerulus (data not shown).

Type-C sensilla

The physiology of *H. subflexa* type-C sensilla is characterized by differential activity profiles of 2 cocompartmentalized, pheromone odorant–sensitive neurons (Baker et al. 2004). Stimulation with the minor pheromone component Z11-16:OH elicits activity from an ORN exhibiting smaller action potentials, whereas larger action potentials are generated from the second ORN upon stimulation with either Z11-16:Ac or Z9-14:Ald (Figure 7A) (Baker et al. 2004). We obtained 19 successfully stained type-C sensillar preparations out of 23 attempts. Seventeen of these (89.5%) exhibited 2 stained axons projecting to the AM and VM glomeruli, the 2 smaller glomeruli of the MGC (Table 1; Figures 2, 7B,C, and 8A). The remaining 2 preparations resulted in a single stained axon projecting to the VM glomerulus. Three of these 17 exhibited additional stained axons targeting 1 or 2 ordinary glomeruli (Table 1; Figure 8B,C). There appeared to be no differential activity-dependent ORN cobalt uptake resulting from stimulation with either 10 μg Z11-16:Ac or 10 μg Z11-16:OH.

Discussion

We have now described the pathways of axons from *H. subflexa* pheromone component–tuned ORNs residing in trichoid sensilla to their glomerular destinations in the antennal lobe.

Table 1 Summary of the glomerular arborization destinations of 3 different types of ORNs in male *Heliothis subflexa* sensilla

Target glomeruli	Stained sensilla	Percentage	
A-type (*N* = 28)			
Single target			
Cu	17	60.7	
Multiple targets			
Cu + PCx1	11	39.3[a]	
B-type (*N* = 28)			
Single target			
DM	4	14.3	17.9
PCx4	1	3.6	
Multiple targets			
DM + PCx4	18	64.3	
DM + PCx4 + Ord(s)	4	14.3	82.1
DM + PCx4 + Cu	1	3.6	
C-type (*N* = 19)			
Single target			
VM	2	10.5	10.5
AM	0	0	
Multiple targets			
VM + AM	14	73.7	89.5
VM + AM + Ord(s)	3	15.8	

[a]Two of these occasions also stained ordinary glomeruli and one occasion also stained PCx4 in addition to the Cu and PCx1.

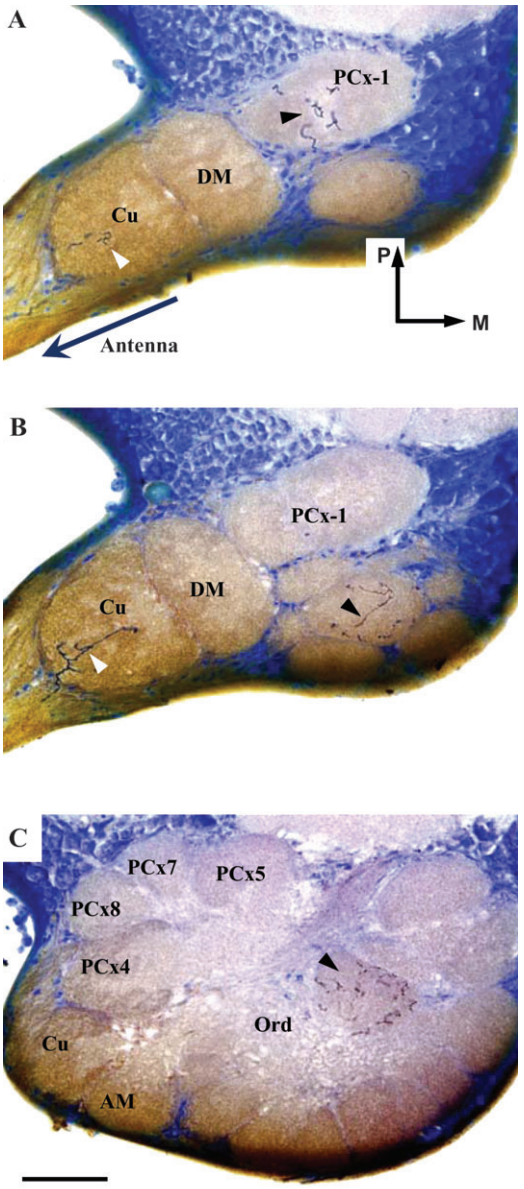

Figure 4 Dorsal views of stained neuronal arborization from a type-A sensillum. **(A)** A section at approximately 30 μm depth from the most dorsal surface. Axonal arborizations can be seen in PCx1 (black arrowhead) and the Cu (light arrowhead). **(B)** The next section, 10 μm more ventral than (A), shows an extensive axonal arborization in the Cu (light arrowhead) and a second stained axon projecting to an ordinary glomerulus (black arrowhead) situated near the DM glomerulus of the MGC. **(C)** A section at a depth 40 μm more ventral than (B) showing another stained axon (arrowhead) terminating in a second ordinary glomerulus. Ord, ordinary glomeruli; P, posterior; M, Medial. Scale bar = 50 μm.

When we couple our findings with those of Vickers and Christensen (2003), who described pheromone component–specific projection interneuron arborizations into each of the 4 *H. subflexa* MGC compartments, we conclude that there is a correspondence between pheromone odorant–specific input to, and output from, the different MGC compartments. These relationships for *H. subflexa* are depicted in Figure 9A.

Although large numbers of our single-sensillar preparations exhibited 2 stained ORNs each projecting to a different glomerulus, the ORNs reached the same glomeruli with high fidelity from preparation to preparation. Pairs of glomeruli exhibiting stained axons were nearly perfectly correlated with their origin from type-A, type-B, or type-C sensilla. Preparations exhibiting only single stains were similarly highly correlated with their sensillar-type origin.

Sixty percent of the type-A sensillar preparations showed a single stained ORN projecting its axon without exception to the Cu. Another 40% of type-A sensillar preparations had 2 stained ORNs, with all these preparations exhibiting an ORN arborization in the Cu, plus a second stained axon targeting the PCx1 glomerulus of the PCx. No pheromone component–sensitive ORN in moths has ever been found to arborize anywhere but in the MGC, and we conclude that it is the Z11-16:Ald–tuned ORNs from these preparations that target the Cu.

This interpretation is consonant with what has been shown for the projections of Z11-16:Ald–tuned ORNs in *H. virescens* and *H. zea* (Berg et al. 1998; Lee et al. 2006). In addition,

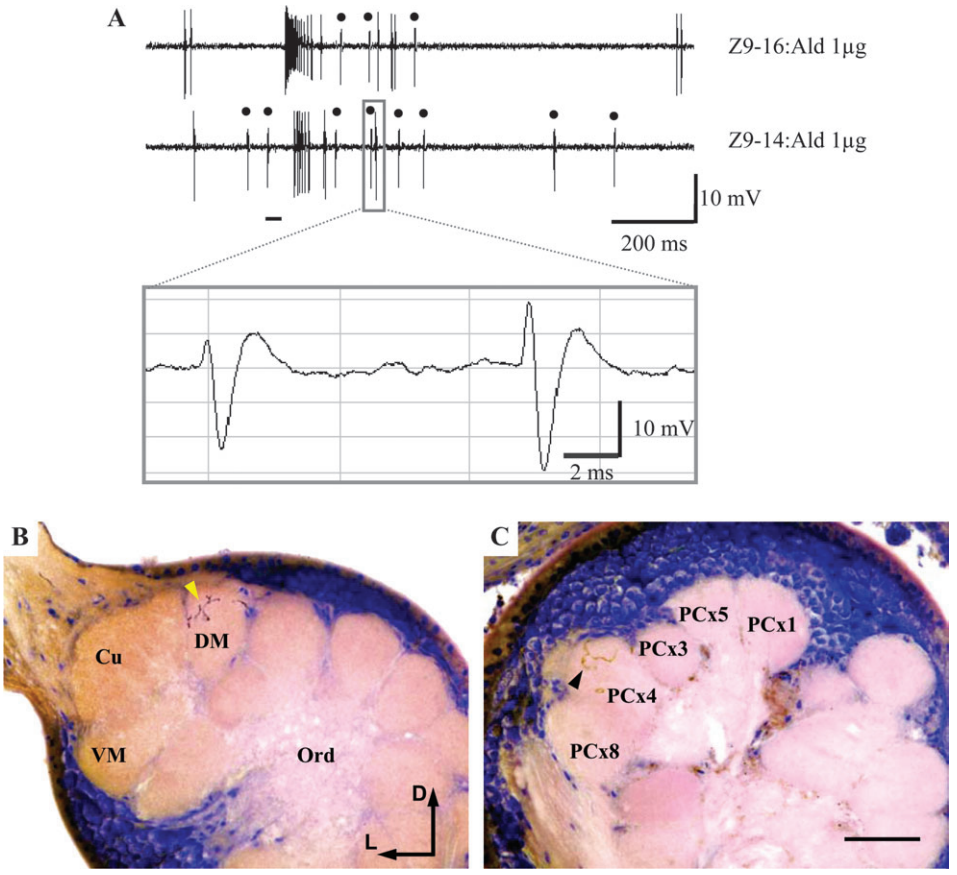

Figure 5 **(A)** Responses of an ORN from a type-B sensillum. This larger spiking ORN with a fairly symmetrically bipolar waveform is responsive to stimulation with Z9-16:Ald and Z9-14:Ald. Other test compounds did not evoke any neuronal responses. Asymmetric waveforms of the action potentials from the second, smaller spiking neuron (black dots) were spontaneously generated; this neuron did not respond to any of the compounds tested. Inset shows waveforms from 2 different neurons in extended time scale. **(B–C)** Frontal sections showing neuronal projection patterns of the 2 ORNs housed within a type-B sensillum. (B) A section at about 90 µm depth from the frontal surface of the antennal lobe revealed an axonal arborization in the DM glomerulus of the MGC (arrowhead). (C) A section 90 µm posterior to (B) showing a second axon arborizing in the PCx4 glomerulus (arrowhead). Ord, ordinary glomeruli; D, dorsal; L, lateral. Scale bar = 50 µm.

projection interneuron–staining patterns in the *H. subflexa* antennal lobe (Vickers and Christensen 2003) show definitively that the Cu is where Z11-16:Ald–tuned projection interneurons arborize. Given the linear pathways of ORN to glomerulus to projection interneuron that have been found in *H. virescens* and *H. zea* (Figure 9; Berg et al. 1998; Vickers et al. 1998; Lee et al. 2006), this again indicates that the Z11-16:Ald–tuned ORNs arborize in the Cu of the *H. subflexa* MGC.

The colocalized ORNs from type-A sensilla are therefore the ones in our cobalt stains that target the PCx1 glomerulus in the newly described PCx. The targeting of the PCx by the cocompartmentalized ORNs in type-A sensilla was definitively shown in *H. zea* (Lee et al. 2006). One of the most striking results from the current study is the finding that the ORNs in *H. subflexa* that are cocompartmentalized with pheromone component–sensitive ORNs in either type-A or type-B sensilla project reliably into their own specific glomeruli in a cluster of glomeruli having a morphology similar to the PCx of *H. zea* (Figure 9A,C; Lee et al. 2006). Moreover, as in *H. zea*, the colocalized, very small–spiking ORNs in type-A sensilla in *H. subflexa* (Figure 3A) always project into the most dorsal and medial of the 8 PCx glomeruli in *H. subflexa*, which we have labeled, as in *H. zea*, the PCx1 (Lee et al. 2006). Again as in *H. zea*, the PCx1-targeting neurons in *H. subflexa* were not found originating from any sensilla other than type-A; we conclude that these ORNs are not arbitrarily cocompartmentalized with the larger spiking ORNs in type-A sensilla.

Although the colocalized ORNs in type-A sensilla did not respond to any general odorants or pheromone-related analogs from a panel of more than 70 odorants (Lee 2006), we did see activity from this small-spiking ORN whenever there was firing from the large-spiking ORN in response to Z11-16:Ald or a structurally similar analog (Lee 2006).

We also tried stimulation with the C16 acids corresponding to the enzymatic degradation products of heliothine aldehyde pheromone components (Prestwich et al. 1989; Tasayco and Prestwich 1990a, 1990b) because in other noctuid species such as *Trichoplusia ni* and *Agrotis segetum*, the ORNs that

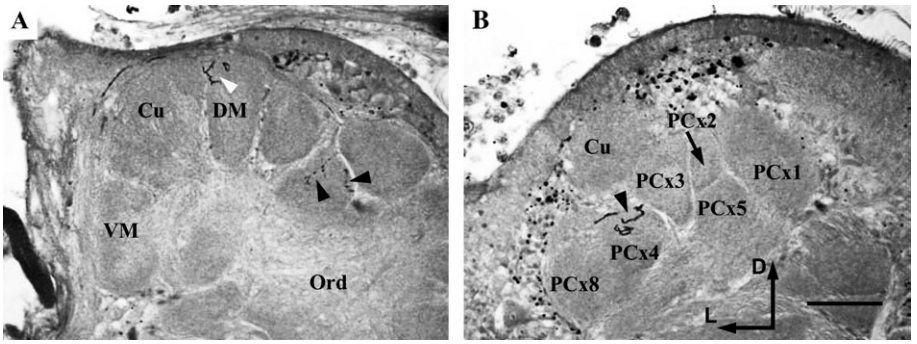

Figure 6 Frontal sections showing neuronal projection patterns of a type-B sensillar neuron that projects to an ordinary glomerulus in addition to neurons projecting to the DM and PCx4. **(A)** One axon arborized in the DM glomerulus (light arrowhead), and another arborized in the water drop–shaped ordinary glomerulus (black arrowheads). **(B)** Another stained axon arborizing in the PCx4 (arrowhead) at a depth 80 μm more posterior to (A). Ord, ordinary glomeruli; D, dorsal; L, lateral. Scale bar = 50 μm.

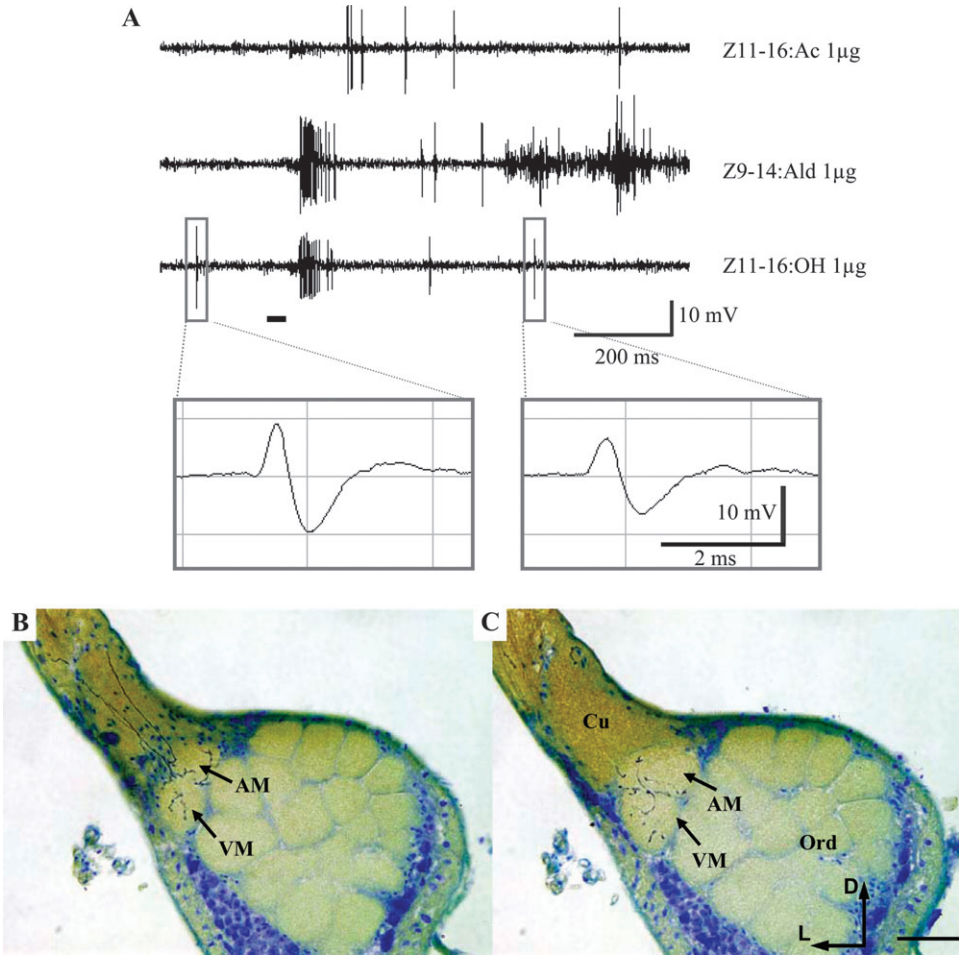

Figure 7 **(A)** Spike trains of ORNs from a type-C sensillum. The tracings show a larger amplitude spiking ORN that responds to both Z11-16:Ac and Z9-14:Ald and a smaller amplitude spiking ORN that responds to Z11-16:OH. Insets show waveforms from larger and smaller spiking ORNs in extended time scale. **(B)** Frontal section showing axonal projections and arborizations of the ORNs in the AM and VM glomeruli (arrows). **(C)** A section 10 μm more posterior to (B) showing arborizations in the AM and VM glomeruli. Ord, ordinary glomeruli; D, dorsal; L, lateral. Scale bar = 50 μm.

are cocompartmentalized with major component-sensitive ORNs (Hansson et al. 1992; Todd et al. 1992, 1995) are highly responsive to the corresponding degradation products (alcohols) of the acetate major component (Prestwich et al. 1989). None of this large array of odorants evoked responses from the colocalized ORN; the correspondence of firing

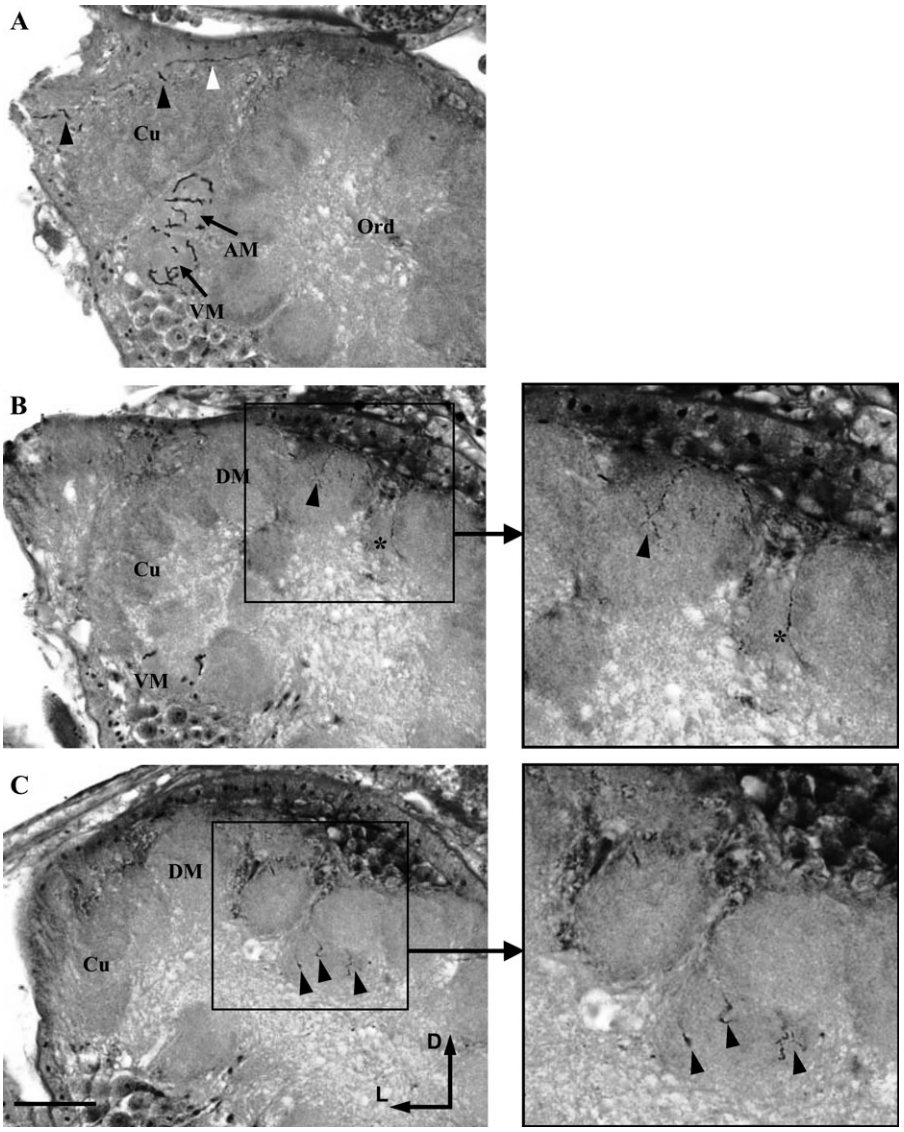

Figure 8 Frontal sections showing neuronal projection patterns of type-C sensillar neurons that project to ordinary glomeruli in addition to those having arborizations in the AM and VM glomeruli. **(A)** Arborizations in the AM and VM glomeruli (arrows). Two axonal projections to VM and AM each are visible on dorsal to the Cu (black arrowheads). A faint axonal projection to an ordinary glomerulus is also visible close to the dorsal AL surface (light arrowhead). **(B)** A section 40 μm posterior to (A) showing remains of arborizations in the VM glomerulus but in addition with a third axon arborizing in an ordinary glomerulus (arrowhead) situated adjacent to the DM glomerulus. A fourth axon shows its projection (asterisk) to its target glomerulus. Inset: magnified image showing arborization (arrowhead) as well as projection of fourth axon (asterisk). **(C)** Section approximately 40 μm posterior to (B) showing this fourth axonal arborization (arrowheads) in the water drop–shaped ordinary glomerulus. Inset: magnified image of the target glomerulus. Ord, ordinary glomeruli; D, dorsal; L, lateral. Scale bar = 50 μm.

between the large-spiking and small-spiking ORNs was clear, however (Lee 2006). The anatomical conformity of the target glomeruli of the colocalized ORNs in type-A sensilla of these North American heliothine moths implies that if there is any odorant-specific processing performed within the PCx1, it may be similar across heliothine species. We have pointed out previously (Lee et al. 2006) the morphological similarities of the PCx we described in *H. zea* to glomeruli that have previously been labeled ''ordinary'' in *H. virescens* and *H. assulta*; all receiving input from cocompartmentalized ORNs having unknown tuning properties (Berg et al. 1998, 2005). In Figure 9, we have summarized the current status of ORN input projections to the MGC and PCx for these 4 species of heliothine moth.

Although there were 2 ORNs consistently stained in type-B sensilla with one projecting to the DM and the other to the PCx4, we conclude that the DM glomerulus receives input from Z9-16:Ald–tuned ORNs because in moths no pheromone component–sensitive ORNs, and only rarely projection interneurons, have been found to arborize outside of

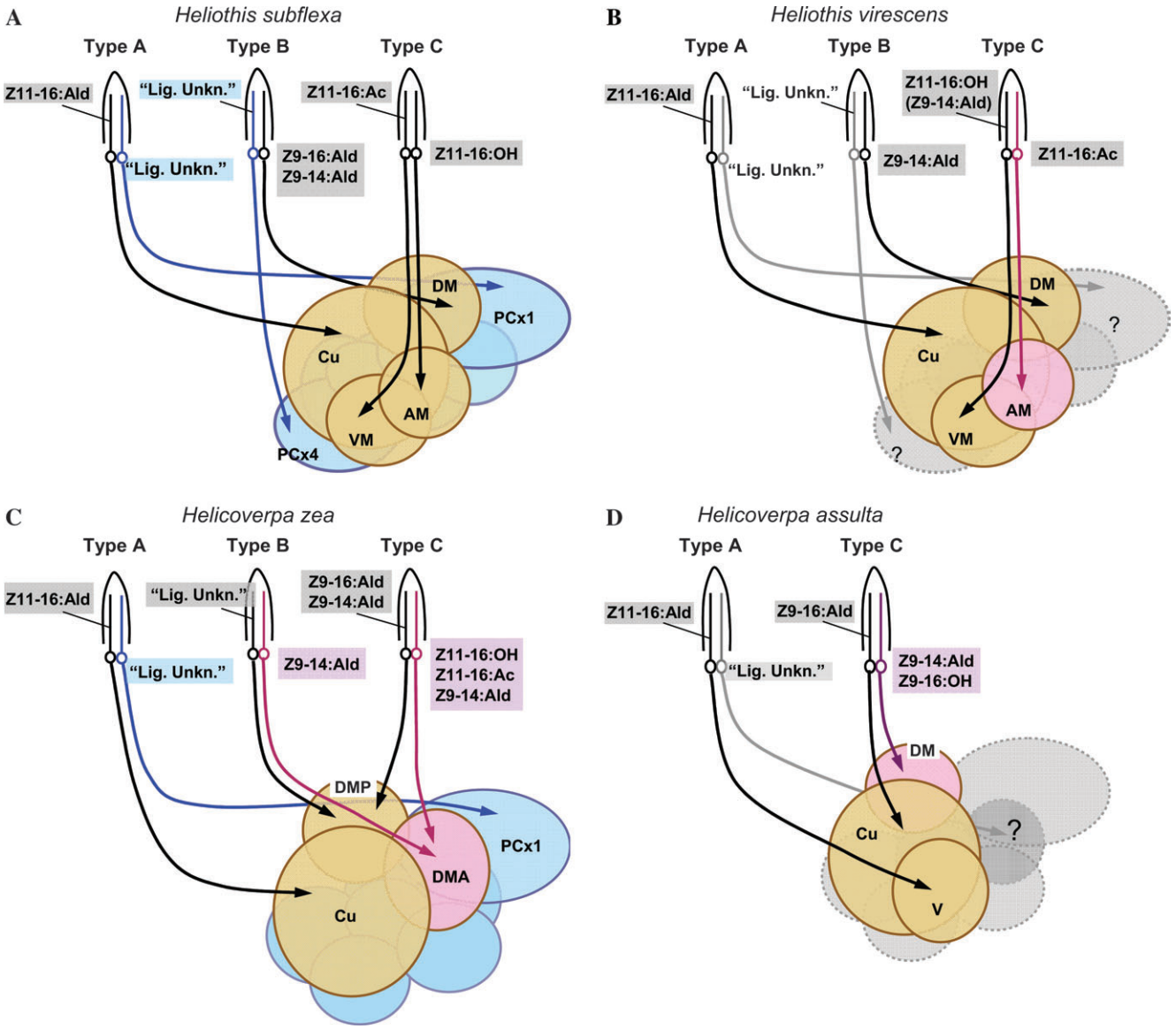

Figure 9 Diagrams of the sensillar compartmentalization arrangements and projection destinations of ORNs in type-A, B, and C trichoid sensilla of 4 heliothine moth species. The schemes follow the results of studies using cobalt staining of physiologically characterized neurons within specific sensilla (Berg et al. 1998, 2005; Lee et al. 2006; Lee et al., this paper), staining of characterized projection interneurons (Vickers et al. 1998, Vickers and Christensen 2003), and also additional results from calcium imaging (Galizia et al. 2000; Lee et al. 2006). Glomeruli in gold are MGC glomeruli known to be involved in pheromonal attraction. Glomeruli in pink are MGC glomeruli known to be involved in behavioral antagonism. Glomeruli in blue are those known through anatomical analyses to reside in the PCx, and those in gray are speculated to reside in a PCx that has not been anatomically characterized yet. **(A)** *Heliothis subflexa* (this paper) showing pheromone component–responsive ORNs (black axons) projecting to their respective MGC glomeruli and the cocompartmentalized ORNs from types A and B sensilla (blue axons) projecting to the PCx1 and PCx4 glomeruli, respectively. **(B)** *Heliothis virescens* (Berg et al. 1998; Galizia et al. 2000) showing pheromone component–responsive ORNs projecting to respective MGC glomeruli. We speculate from the reports of Berg et al. (1998, 2002) that cocompartmentalized neurons from type-A and type-B sensilla (gray axons) project to PCx1 and PCx4 glomeruli (in gray) that have not been characterized as such as they have for *H. subflexa*. **(C)** *Helicoverpa zea* (Lee et al. 2006). The significant features of this projection pattern include the projection of the secondary ORN in type-A sensilla to the PCx1 and also the finding that the ORNs in type-B sensilla project to the same MGC glomeruli as the ORNs from type-C sensilla but type-B ORNs do not respond to pheromone compounds except for Z9-14:Ald. **(D)** *Helicoverpa assulta* (Berg et al. 2005), in which the major pheromone component is Z9-16:Ald, and the ORNs tuned to this component project to the Cu. ORNs tuned to the minor component, Z11-16:Ald, project from their type-A sensilla to the ventral (V) glomerulus in the MGC. We speculate from Berg et al. (2002, 2005) that the secondary ORN from type-A sensilla (gray axon) arborizes in a PCx glomerulus that has not yet been anatomically characterized (in gray). DMA, dorsomedial anterior glomerulus; DMP, dorsomedial posterior glomerulus; V, ventral glomerulus; Lig. Unkn., ligand unknown.

the MGC (Hansson and Christensen 1999; Vickers and Christensen 2003). This assignment is also consonant with the arborization of Z9-16:Ald–responsive projection interneurons that always target the DM glomerulus (Vickers and Christensen 2003). In addition, calcium images we have started to accumulate for *H. subflexa* show that the focal point of calcium activity in response to Z9-16:Ald antennal stimulation is in the DM glomerulus (MA Carlsson, BS Hansson, S-G Lee, TC Baker, unpublished data). There is thus a linear arrangement through the DM glomerulus of Z9-16:Ald–related input from ORNs and Z9-16:Ald–related output from projection interneurons. The PCx4 glomerulus of *H. subflexa* is therefore functionally and morphologically engaged in receiving information from the ORN that is colocalized in type-B sensilla with the ORN responsive to Z9-16:Ald/Z9-14:Ald. This companion ORN did not respond consistently to any of the approximately 70 test compounds with which it was challenged (Lee 2006). This type-B colocalized ORN produces spontaneous asymmetric action potentials, and the identical waveform of this type of ORN across all the type-B sensilla we recorded from suggests that it has a distinctive signal-generating system that is different from that of the Z9-16:Ald/Z9-14:Ald–responsive ORN in terms of its ion channel characteristics, especially during the outward current of hyperpolarization.

In *H. virescens*, one of 2 preparations of Berg et al. (1998) for the staining of type-B sensilla containing Z9-14:Ald–responding ORNs showed one axon projecting to an ''ordinary glomerulus'' located ventral to the MGC, in addition to an ORN projecting to the DM compartment of the MGC. The DM glomerulus was concluded to be the location receiving Z9-14:Ald–related input based, among other factors, on the DM arborization location of Z9-14:Ald–tuned projection interneurons (Vickers et al. 1998). Subsequently, a calcium imaging study confirmed the *H. virescens* DM glomerulus as the MGC glomerulus receiving ORN excitation related to Z9-14:Ald (Galizia et al. 2000). The ordinary glomerulus that is depicted in Berg et al. (1998) displays a similar, topographic, ventral proximity to the PCx4 glomerulus of *H. subflexa* (Figure 9A,B). No mention was made of the posterior depth of this glomerulus in relation to the DM glomerulus (Berg et al. 1998). The colocalized ORN that targets it has an undefined tuning profile because no compound was found that excited it (Berg et al. 1998).

The projections of the ORNs we found in type-C sensilla exhibit highly consistent patterns of labeling into the AM and VM, the 2 smaller glomeruli in the MGC. We were not able to directly identify which of these 2 ORNs target the AM or the VM glomerulus due to the nonselectivity of cobalt dye uptake during cobalt application. However, the arborization of a Z11-16:OH-responsive projection interneuron in the AM glomerulus (Vickers and Christensen 2003) and the increasingly well-established linearity of pheromone component olfactory pathways in heliothine moths (Berg et al. 1998; Vickers et al. 1998; Vickers and Christensen 2003) suggest that the AM glomerulus is the primary receiving center for action potentials from Z11-16:OH–tuned ORNs. By default, the VM glomerulus should be the target glomerulus for the ORN that responds to Z11-16:Ac and Z9-14:Ald. The first calcium images from *H. subflexa* now also support this assignment (MA Carlsson, BS Hansson, S-G Lee, TC Baker, unpublished data).

The frequency with which ordinary glomeruli received stains from third or fourth ORNs residing in *H. subflexa* types A, B, and C long trichoids was higher in *H. subflexa* than in other heliothines. This would imply that in this species, there may be more ORNs tuned to general odorants that are cocompartmentalized in these sensilla with ORNs tuned to pheromone components than there are in either *H. zea* (Lee et al. 2006) or *H. virescens* (Berg et al. 1998). The ordinary glomerulus staining ORNs arose with similar likelihood from type-A, type-B, and type-C sensilla, and so no one type of sensillum was associated with the presence of these ORNs. The stained arborizations were not in a wide variety of ordinary glomeruli but rather were restricted with high fidelity to but a few specific glomeruli. Arborizations of 7 of the 16 ORNs targeting ordinary glomeruli terminated in an ordinary glomerulus most closely adjacent and medial–posterior to the DM (Figures 4B and 8B). In addition, 2 ORNs from type-A, 2 from a type-B, and 3 from a type-C sensillum targeted a water drop–shaped glomerulus situated medially and several tens of micrometers posterior to the ordinary glomerulus mentioned above (Figures 4C, 6A, and 8C). We also found a type-A and a type-B sensillum each having an ORN projecting to the most anterior ordinary glomerulus in the antennal lobe. These results imply that these 16 ORNs terminating in ordinary glomeruli and originating variously from types A, B, and C trichoid sensilla might show 3 distinctive tuning spectra to odorant ligands.

It is unclear why, in addition to the MGC and ordinary glomeruli, that a third subcluster of glomeruli, the PCx, should exist in these heliothine moth species. Such a grouping implies a separate, broad function of this structure, just as the MGC cluster is related to pheromone compound inputs and the large cluster of ordinary glomeruli is related to all other odorant inputs. We have only performed staining experiments on physiologically identified ORNs in males of these species thus far. We hope to perform similar studies and find sensilla in females that have Z11-16:Ald–responsive ORNs in order to try staining any cocompartmentalized ORNs to determine their target glomeruli in the female antennal lobe. Our preliminary analysis of the female antennal lobes of *H. zea* and *H. subflexa* has thus far revealed a structure in both species similar to the male PCxs but appearing slightly different than those of the males. A more thorough morphological sex-specific comparison coupled with physiological and cobalt-staining studies using females should help provide more insight regarding any functional and morphological dimorphisms of the PCx in these species.

Acknowledgements

This study was funded by grant #2003-01471 from the US Department of Agriculture NRI program to TCB. We thank to Drs J.C. Fiala and K.M. Harris for image analysis software.

References

Almaas TJ, Christensen TA, Mustaparta H. 1991. Chemical communication in heliothine moths. I. Antennal receptor neurons encode several features of intra- and interspecific odorants in the male corn earworm moth *Helicoverpa zea.* J Comp Physiol A 169:249–58.

Bacon JB, Altman JS. 1977. A silver-intensification method for cobalt-filled neurons in wholemount preparations. Brain Res 138:359–63.

Baker TC, Ochieng SA, Cossé AA, Lee S-G, Todd JL, Quero C, Vickers NJ. 2004. A comparison of responses from olfactory receptor neurons of *Heliothis subflexa* and *Heliothis virescens* to components of their sex pheromone. J Comp Physiol A 190:155–65.

Bennett HS, Wyrick AD, Lee SW, McNeil JH Jr. 1976. Science and art in preparing tissues embedded in plastic for light microcopy, with special reference to glycol methacrylate, glass knives and simple stains. Stain Technol 51:71–97.

Berg BG, Almaas TJ, Bjaalie JG, Mustaparta H. 1998. The macroglomerular complex of the antennal lobe in the tobacco budworm *Heliothis virescens*: specified subdivision in four compartments according to information about biologically significant compounds. J Comp Physiol A 183: 669–82.

Berg BG, Almaas TJ, Bjaalie JG, Mustaparta H. 2005. Projections of male-specific receptor neurons in the antennal lobe of the oriental tobacco budworm moth, *Helicoverpa assulta*: a unique glomerular organization among related species. J Comp Neurol 486:209–20.

Berg BG, Galizia CG, Brandt R, Mustaparta H. 2002. Digital atlases of the antennal lobe in two species of tobacco budworm moths, the oriental *Helicoverpa assulta* (male) and the American *Heliothis virescens* (male and female). J Comp Neurol 446:123–34.

Berg BG, Tumlinson JH, Mustaparta H. 1995. Chemical communication in heliothine moths IV. Receptor neuron responses to pheromone compounds and formate analogues in the male tobacco budworm moth *Heliothis virescens.* J Comp Physiol A 177:527–34.

Cho S, Mitchell A, Regier JC, Mitter C, Poole RW, Firedlander TP, Zhao S. 1995. A highly conserved nuclear gene for low-level phylogenetics: elongation factor-1α recovers morphology-based tree for heliothine moths. Mol Biol Evol 12:650–6.

Christensen TA, Mustaparta H, Hildebrand JG. 1991. Chemical communication in heliothine moths. II. Central processing of intra- and interspecific olfactory messages in the corn earworm moth *Helicoverpa zea.* J Comp Physiol A 169:259–74.

Christensen TA, Mustaparta H, Hildebrand JG. 1995. Chemical communication in heliothine moths. VI. Parallel pathways for information processing in the macroglomerular complex of the tobacco budworm moth *Heliothis virescens.* J Comp Physiol A 177:545–557.

Cossé AA, Todd JL, Baker TC. 1998. Neurons discovered in male *Helicoverpa zea* antennae that correlate with pheromone-mediated attraction and interspecific antagonism. J Comp Physiol A 182:585–94.

Fang QQ, Cho W, Regier JC, Mitter C, Matthews M, Poole RW, Firedlander TP, Zhao S. 1997. A new nuclear gene for insect phylogenetics: dopa decarboxylase is informative of relationships within Heliothinae (Lepidoptera: Noctuidae). Syst Biol 46:269–83.

Galizia CG, Sachse S, Mustaparta H. 2000. Calcium responses to pheromones and plant odours in the antennal lobe of the male and female moth *Heliothis virescens.* J Comp Physiol A 186:1049–63.

Hansson BS. 1995. Olfaction in Lepidoptera. Experientia 51:1003–27.

Hansson BS, Almaas TJ, Anton S. 1995. Chemical communication in heliothine moths V. Antennal lobe projection patterns of pheromone-detecting olfactory receptor neurons in the male *Heliothis virescens* (Lepidoptera: Noctuidae). J Comp Physiol A 177:535–43.

Hansson BS, Christensen TA. 1999. Functional characteristics of the antennal lobe. In: Hansson BS, editor. Insect olfaction. New York: Springer. p 126–61.

Hansson BS, Ljungberg H, Hallberg E, Lofstedt C. 1992. Functional specialization of olfactory glomeruli in a moth. Science 256:1313–5.

Heath RR, McLaughlin JR, Proshold F, Teal PEA. 1991. Periodicity of female sex pheromone titer and release in *Heliothis subflexa* and *H. virescens* (Lepidoptera: Noctuidae). Ann Entomol Soc Am 84:182–9.

Heath RR, Mitchell ER, Cibrian-Tovar J. 1990. Effect of release rate and ratio of (*Z*)-11-hexadecen-1-ol from synthetic pheromone blends on trap capture of *Heliothis subflexa* (Lepidoptera: Noctuidae). J Chem Ecol 16:1259–68.

Kaissling KE. 1974. Sensory transduction in insect olfactory receptors. In: Jaenicke L, editor. Biochemistry of sensory functions. Berlin, Germany: Springer-Verlag. p 243–73.

Klun JA, Leonhardt BA, Lopez JD Jr, Lachance LE. 1982. Female *Heliothis subflexa* (Lepidoptera: Noctuidae) sex pheromone: chemistry and congeneric comparisons. Environ Entomol 11:1084–90.

Klun JA, Plimmer JR, Bierl-Leonhardt BA, Sparks AN, Chapman OL. 1979. Trace chemicals: the essence of sexual communication systems in *Heliothis* species. Science 204:1328–30.

Klun JA, Plimmer JR, Bierl-Leonhardt BA, Sparks AN, Primiani M, Chapman OL, Lee GH, Lepone G. 1980. Sex pheromone chemistry of female corn earworm moth, *Heliothis zea.* J Chem Ecol 6:165–75.

Laster ML. 1972. Interspecific hybridization of *Heliothis virescens* and *H. subflexa.* Environ Entomol 1:682–7.

Lee S-G. 2006. Pheromone-related olfactory neuronal pathways of male heliothine moths [PhD thesis]. University Park, PA: The Pennsylvania State University. p 120–66.

Lee S-G, Carlsson MA, Hansson BS, Todd JL, Baker TC. 2006. Functional organization of the antennal lobe of the moth, *Helicoverpa zea.* J Comp Physiol A 192:351–63.

Mitter C, Poole RW, Matthews M. 1993. Biosystematics of the Heliothinae (Lepidoptera: Noctuidae). Annu Rev Entomol 38:207–25.

Ochieng SA, Anderson P, Hansson BS. 1995. Antennal lobe projection patterns of olfactory receptor neurons involved in sex pheromone detection in *Spodoptera littoralis* (Lepidoptera: Noctuidae). Tissue Cell 27:221–32.

Ochieng SA, Baker TC. 2002. Host plant volatiles synergize responses of sex pheromone-specific olfactory receptor neurons in male *Helicoverpa zea.* J Comp Physiol A 188:325–33.

Pope MM, Gaston LK, Baker TC. 1984. Composition, quantification, and periodicity of sex pheromone volatiles from individual *Heliothis zea* females. J Insect Physiol 30:943–5.

Prestwich GD, Graham SMcG, Handley M, Latli B, Streinz L, Tasayco ML. 1989. Enzymatic processing of pheromones and pheromone analogs. Experientia 45:263–70.

Quero C, Baker TC. 1999. Antagonistic effect of (*Z*)-11-hexadecen-1-ol on the pheromone-mediated flight of *Helicoverpa zea* (Boddie) (Lepidoptera: Noctuidae). J Insect Behav 12:701–9.

Roelofs WL, Hill AS, Cardé RT, Baker TC. 1974. Two sex pheromone components of the tobacco budworm moth, *Heliothis virescens.* Life Sci 14:1555–62.

Shaver TN, Lopez JD Jr, Hartstack AW Jr. 1982. Effects of pheromone components and their degradation products on the response of Heliothis spp. to traps. J Chem Ecol 8:755–62.

Sheck AL, Gould F. 1995. Genetic analysis of differences in oviposition preferences of *Heliothis virescens* and *H. subflexa* (Lepidoptera: Noctuidae). Environ Entomol 24:341–7.

Sheck AL, Gould F. 1996. The genetic basis of differences in growth and behavior of specialist and generalist herbivore species: selection on hybrids of *Heliothis virescens* and *Heliothis subflexa* (Lepidoptera). Evolution 50:831–41.

Tasayco ML, Prestwich GD. 1990a. Aldehyde oxidases and dehydrogenases in antennae of five moth species. Insect Biochem 20:691–700.

Tasayco ML, Prestwich GD. 1990b. Aldehyde-oxidazing enzymes in an adult moth: in vitro study of aldehyde metabolism in *Heliothis virescens.* Arch Biochem Biophys 278:444–51.

Teal PEA, Heath RR, Tumlinson JH, McLaughlin JR. 1981. Identification of a sex pheromone of *Heliothis subflexa* (Gn.) (Lepidoptera: Noctuidae) and field trapping studies using different blends of components. J Chem Ecol 7:1011–22.

Teal PEA, Oostendorp A. 1995. Effect of interspecific hybridization between *Heliothis virescens* and *H. subflexa* (Lepidoptera: Noctuidae) on sex pheromone production by females. J Insect Physiol 41:519–25.

Todd JL, Anton S, Hansson BS, Baker TC. 1995. Functional organization of the macroglomerular complex related to behaviorally expressed olfactory redundancy in male cabbage looper moths. Physiol Entomol 20:349–61.

Todd JL, Haynes KF, Baker TC. 1992. Antennal neurons specific for redundant pheromone components discovered in normal and mutant *Trichoplusia ni* males. Physiol Entomol 17:183–92.

Tumlinson JH, Hendrichks DE, Mitchell ER, Doolittle RE, Brennan MM. 1975. Isolation, identification, and synthesis of the sex pheromone of the tobacco budworm. J Chem Ecol 1:203–14.

Van der Pers JNC, Den Otter CJ. 1978. Single cell responses from olfactory receptors of small ermine moths to sex-attractants. J Insect Physiol 24:337–43.

Vetter RS, Baker TC. 1984. Behavioral responses of male *Heliothis zea* moths in sustained flight-tunnel to combinations of four compounds identified from female sex pheromone gland. J Chem Ecol 10: 193–202.

Vickers NJ. 2002. Defining a synthetic pheromone blend attractive to male *Heliothis subflexa* under wind tunnel conditions. J Chem Ecol 28:1255–67.

Vickers NJ, Christensen TA. 2003. Functional divergence of spatially conserved olfactory glomeruli in two related moth species. Chem Senses 28:325–38.

Vickers NJ, Christensen TA, Hildebrand JG. 1998. Combinatorial odor discrimination in the brain: attractive and antagonist odor blends are represented in distinct combinations of uniquely identifiable glomeruli. J Comp Neurol 400:35–56.

Accepted July 27, 2006